Magnetic structure, magnetostriction, and magnetic transitions of the Laves-phase compound $NdCo_2$

Z. W. Ouyang,[1] F. W. Wang,[1] Q. Huang,[2] W. F. Liu,[1] Y. G. Xiao,[1] J. W. Lynn,[2] J. K. Liang,[1,3] and G. H. Rao[1,*]
[1]*Beijing National Laboratory for Condensed Matter Physics, Institute of Physics, Chinese Academy of Sciences, Beijing 100080, People's Republic of China*
[2]*NIST Center for Neutron Research, National Institute of Standards and Technology, Gaithersburg, Maryland 20899, USA*
[3]*International Center for Materials Physics, Academia Sinica, Shenyang 110016, People's Republic of China*
(Received 26 August 2004; revised manuscript received 29 November 2004; published 18 February 2005)

The crystal and the magnetic structures as well as magnetostriction of the Laves-phase compound $NdCo_2$ are investigated by means of temperature-dependent high-resolution neutron-powder diffraction. The compound crystallizes in the cubic Laves phase $C15$ structure at high temperature, undergoes a tetragonal distortion (space group $I4_1/amd$) around $T_C \approx 100$ K and an orthorhombic distortion (space group $Fddd$) at $T \approx 42$ K. The temperature dependence of lattice constants, magnetostriction constant, and magnetic moment indicate that the magnetic and structural transitions are second order in the vicinity of T_C and are first-order around 42 K. Refinements of magnetic structure reveal that the Nd moment distinctly exhibits an abrupt increase at the first-order transition and the easy magnetization direction of the compound changes from [001] in the tetragonal lattice to [011] in the orthorhombic lattice, indicating a strong coupling between crystal structure and magnetic properties at zero field. Analysis of the temperature dependence of bondlength suggests a strong magnetic exchange striction in the tetragonal structure and that the abrupt increase of the Nd moment is attributed essentially to a change in crystal electric field. Field-dependent neutron diffraction reveals a decoupling of the magnetic and structural transitions under relatively modest magnetic fields.

DOI: 10.1103/PhysRevB.71.064405 PACS number(s): 75.25.+z, 75.30.Kz, 75.80.+q

I. INTRODUCTION

For more than twenty years the cubic Laves-phase compounds RCo_2 (R=rare earth) have been interesting in condensed matter physics as one of the $4f$-$3d$ systems that show a magnetic instability of the $3d$ subsystem. Owing to the simple magnetic and crystallographic structures of RCo_2, it is possible to give a clear interpretation of most experiments and to check various physical theories.[1] RCo_2 compounds exhibit a number of characteristic properties, in particular a metamagnetic transition induced by an external magnetic field or by the molecular field.[2–6] A large magnetovolume effect that accompanies the magnetic ordering of the itinerant electron system has been observed in many of these compounds. Strong anisotropic magnetoelastic interactions result in various lattice distortions at the magnetic ordering temperature of the RCo_2 compounds and the character of the unit cell distortion is determined by the orientation of the easy axis of the magnetization in all cases.[7] Among the RCo_2 compounds, $NdCo_2$ and $HoCo_2$ unusually exhibit another structural transition at low temperature, in addition to the one taking place at T_C.[7,8]

X-ray diffraction (XRD) analysis revealed that $NdCo_2$ crystallized in the Laves-phase $C15$ structure above Curie temperature $T_C \sim 100$ K, in a tetragonal structure below T_C and in an orthorhombic structure below 42 K.[7,8] Mössbauer study revealed that the easy magnetization direction is along [100] below T_C and changes to [110] of the cubic structure at about 42 K.[9] However, early neutron-powder-diffraction (NPD) studies did not show any change in either the crystalline or the magnetic structure of $NdCo_2$ below its T_C.[10,11] The study of Hendy and Lee[11] did not reveal any noticeable anomaly of the Nd moment in $NdCo_2$ around 42 K, whereas a decrease of Co moment with temperature was shown to occur around 35 K, which was inconsistent with magnetization measurements. Baranov *et al.* observed an abrupt increase of magnetization around 42 K on the magnetization curve of $NdCo_2$ and explained this behavior as a spin reorientation.[12] Normally, a spin-reorientation transition involves exclusively a change in easy direction of magnetization but not in the magnitude of magnetization and crystallographic structure. The XRD work of Ref. 6 demonstrated discontinuous changes of both the lattice constants and the anisotropic magnetostriction constant λ_{100} at 42 K, indicating that the tetragonal to orthorhombic transition is a first-order one. The significant change of crystal structure may alter the electronic structure of the compound accordingly. Therefore, couplings between the crystal structure and magnetic structure are expected, which can lead to changes not only in the easy magnetization direction but also in the Nd and the Co moments, i.e., the magnetic transition at 42 K could be more complex than a simple spin reorientation. Surprisingly, detailed magnetic structure of $NdCo_2$ below 42 K has not been further investigated for more than two decades, though the magnetic structure data is indispensable for constructing a reliable physical model and for understanding the properties of the compound. Thus, the nature of the simultaneous magnetic and structural transitions in $NdCo_2$ at 42 K remains unclear.

The simultaneous occurrence of the first-order structural and magnetic transitions due to the strong magnetoelastic interaction in $NdCo_2$ is intriguing in physics and may be of potential applications. For instance, the coupled first-order magnetic and structural transitions are considered to be re-

sponsible for the giant magnetocaloric effect, the clossal magnetostriction and the giant magnetoresistance in $Gd_5(Si,Ge)_4$ compounds.[13,14] The strong magnetoelastic interaction allows a system to gain magnetic exchange energy at the expense of elastic energy or structure distortion, which could be released by an applied magnetic field as evidenced by the existence of a field-induced monoclinic ferromagnetic phase in $Tb_5Si_2Ge_2$.[15] As for the $NdCo_2$ compound, Baranov *et al.* showed that an applied field greater than 6.5 T could smear out the magnetization jump of the bulk sample at around 42 K.[12] But there is no report regarding the response of the crystal structure to an applied field, i.e., whether the lattice distortion coupled with the magnetic transition at zero field could be released by an applied field.

For the above mentioned reasons, we undertook measurements of the crystal and the magnetic structures of $NdCo_2$ by means of temperature- and field-dependent high-resolution neutron-powder diffraction in order to understand the characters of the magnetic and structural transitions occurring in the compound. In this paper, a brief description of sample preparation and neutron powder diffraction experiments will be given in Sec. II. The crystal and the magnetic structures of $NdCo_2$ in different temperature regions are refined based on NPD data, and the lattice parameters and anisotropic magnetostriction constant of $NdCo_2$ as functions of temperature are derived in Sec. III. A discussion on the correlation between the structural distortion and the magnetic structure is presented in Sec. IV, and a summary is given in Sec. V.

II. EXPERIMENTAL

A polycrystalline sample of $NdCo_2$ was prepared by arc melting the constituent elements with a purity of 99.9% in an atmosphere of high-purity argon. The sample was repeatedly arc melted with the button being turned over. The weight loss during arc melting was less than 0.1 wt. %. The ingots were annealed at 800 °C under vacuum for 14 days. X-ray powder diffraction analysis confirmed that the compound has a cubic Laves-phase *C*15 structure at room temperature. All the neutron experiments were performed at the NIST Center for Neutron Research (NCNR). The magnetic order parameter was determined on the BT-7 spectrometer with a neutron wavelength of 2.4649 Å provided by a pyrolytic graphite monochromator and filter. NPD data for refinement of the crystal and the magnetic structures were collected on the high-resolution, 32-counter BT-1 diffractometer. A Cu (311) monochromator was used to produce a monochromatic neutron beam of wavelength 1.5402(1) Å. Collimators with horizontal divergence of 15, 20, and 7 min of arc were used before and after the monochromator and after the sample, respectively. Data were collected in the 2θ range of 10°–160° with a step of 0.05°. The program FULLPRO[16,17] was used for the Rietveld refinement of the crystal and the magnetic structures of the compound, using the following values of the scattering amplitudes: $b(\mathrm{Nd})=0.769$ and $b(\mathrm{Co})=0.249(\times 10^{-12}$ cm).

III. EXPERIMENTAL RESULTS

A. Crystal and magnetic structures

Typical NPD patterns at different temperatures are presented in Fig. 1, in which the open circles stand for the observed intensities and the solid line is the calculated pattern. The calculated patterns agree well with the experimental ones. A few weak extra peaks are contributed by the Nd_4Co_3 phase, which was included in the refinements. The Bragg peaks above T_C are exclusively nuclear scattering in origin. Figure 2 shows the temperature dependence of intensity of the (111) peak referred to the cubic structure, measured on the BT-7 diffractometer when warming the sample. The Curie temperature derived from Fig. 2 is a little higher than the value determined from magnetization measurement.[18] The curve shown in Fig. 2 mimics the magnetization curve measured by Baranorv *et al.*.[12] The noticeable jump of intensity around 42 K is indicative of the reported spin reorientation.

Because of the exact overlap of magnetic reflections with the nuclear Bragg reflections, the nuclear structure was first refined by using the NPD data in the high angle region where the contribution of magnetic ordering is negligible. The data in the range of $2\theta=60°$–160° were used at this stage for the refinement of nuclear structure. The structural and profile parameters obtained from the refinement were used to derive the profile generated by the nuclear structure. A careful analysis reveals that $NdCo_2$ has the cubic Laves-phase structure with space group $Fd\bar{3}m$ at room temperature. With decreasing temperature, $NdCo_2$ exhibits a tetragonal distortion (space group $I4_1/amd$) when $42<T<T_C\approx 100$ K and an orthorhombic distortion (space group $Fddd$) when $T<42$ K. These results are in good agreement with those revealed by x-ray powder diffraction.[7] Table I gives the structural information of $NdCo_2$. The temperature dependence of the lattice constants and the unit cell volume per chemical formula are showed in Fig. 3. They exhibit continuous changes in the vicinity of T_C but discontinuous changes around 42 K.

After refining the nuclear structure based on the high angle NPD data, the intensities of magnetic reflections were then determined by subtracting the contribution of nuclear structure from the observed intensities. An example of this procedure is illustrated in the inset of Fig. 1 for $T=9$ K. The calculated profile in the upper part (solid line) does not include the magnetic contribution and therefore the difference curve at the bottom shows the magnetic reflections. In $NdCo_2$ the contribution of the magnetic ordering to the neutron diffraction intensity is very small, compared with that of the nuclear scattering. Since the character of the unit cell distortion of RCo_2 compounds is determined by the orientation of the easy axis of magnetization, the easy magnetization direction of $NdCo_2$ is expected to be along [001] for the tetragonal distortion and along [011] for the orthorhombic distortion.[7]

In the present model of magnetic structure used in the refinement, it is assumed that the moments of the magnetic atoms in $NdCo_2$ exhibit a collinear alignment. The initial moments are set to be equal along the *b* and *c* axes in the orthorhombic lattice, i.e., the resultant moment is along the [110] direction in the cubic structure, and set to be along the *c* axis in the tetragonal lattice, i.e., [100] direction in the cubic structure, in accordance with the character of the unit cell distortions. At room temperature the isotropic temperature factors are determined to be $\langle u^2\rangle_{\mathrm{Nd}}\sim 0.0065$ Å^2 and

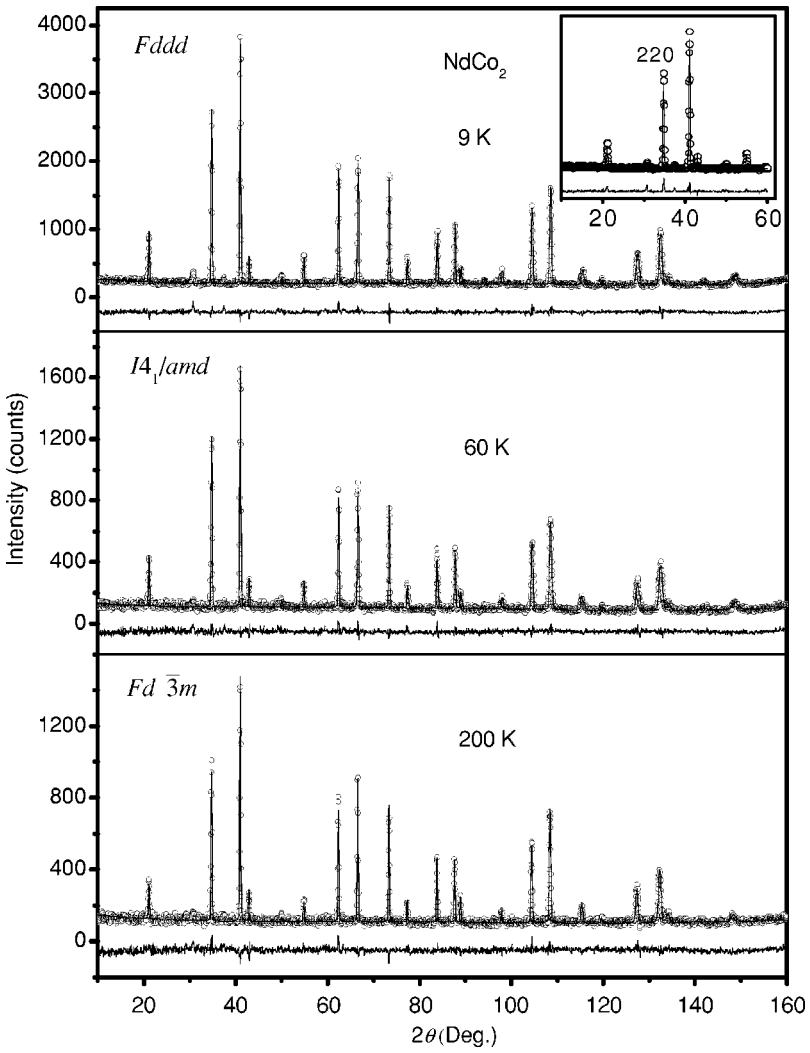

FIG. 1. Typical NPD patterns at 9, 60, and 200 K for $NdCo_2$. The open circles stand for the observed intensities, the solid lines are the calculated profiles. At the bottom is shown the difference between the experimental and calculated intensities. In the inset is shown the calculated pattern without the magnetic contribution in the low angle range. The difference at the bottom represents the contribution of the magnetic structure to the diffraction pattern. The index of the reflections refers to the cubic structure.

$\langle u^2\rangle_{Co} \sim 0.0057$ Å^2. However, with decreasing temperature the refinement of B_{Nd} and B_{Co} exhibits instability because of the small moment of the Co and a strong correlation between the temperature factor B and the magnetic moment of both the Nd and Co atoms. Considering the fact that the temperature factor reduces with decreasing temperature, we approximately assume that both B_{Nd} and B_{Co} decrease linearly from the values at room temperature to zero (or close to zero in this system) at 0 K. The magnetic moments of the Nd and Co atoms at different temperatures are then derived successfully from the refinements and those at 9, 60, and 200 K are listed in Table I. The refinement results of the magnetic structure indicate that the Nd moment and Co moment couple ferromagnetically along the [001] direction in the tetragonal lattice and along the [011] direction in the orthorhombic lattice, in agreement with the general rule of the coupling between light rare-earth metal moment and transition metal moment within the two-sublattice model.[19] At 9 K, the Nd moment is $2.80\mu_B$, close to its free trivalent ion value, and the Co moment is $0.73\mu_B$, in agreement with the molecular-field induced Co moment in RCo_2 documented in Ref. 1. The total magnetic moment of $NdCo_2$ derived from the structure refinement results is about $4.26\mu_B$/f.u. at 9 K, in good agreement with the results of magnetization measurements.[18] The temperature dependence of the magnetic moments is shown in Fig. 4. The moment of Nd atom exhibits an abrupt increase at about 42 K, in coincidence with the BT-7 data shown in Fig. 2 and the magnetization curve reported in Ref.

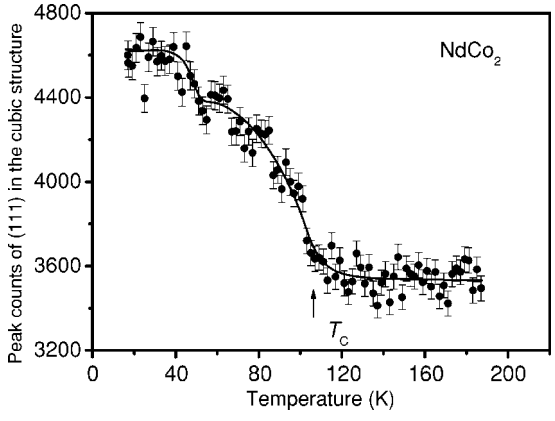

FIG. 2. Temperature dependence of the NPD counts of (111) peak in the cubic structure measured on the BT-7 diffractometer. The errors bars are also shown and represent one standard deviation. The solid curve is a guide to the eye. The arrows indicate the T_C.

TABLE I. Structural parameters of $NdCo_2$ at 9, 60, and 200 K.

Parameters	9 K	60 K	200 K
Structure	Orthorhombic	Tetragonal	Cubic
Space group	*Fddd*	$I4_1/amd$	$Fd\bar{3}m$
a(Å)	7.2974(2)	5.1566(1)	7.2914(2)
b(Å)	7.2821(6)	5.1566(1)	
c(Å)	7.2775(6)	7.2708(3)	
V(Å^3/f.u.)	48.34(1)	48.33(1)	48.46(1)
Nd site	$8a(0,0,0)$	$4b(0,0,1/2)$	$8a(0,0,0)$
$M_x(\mu_B)$	0	0	0
$M_y(\mu_B)$	1.98(4)	0	0
$M_z(\mu_B)$	1.98(4)	2.43(8)	0
Moment(μ_B)	2.80(6)	2.43(8)	0
Co site	$16d(5/8,5/8,5/8)$	$8c(0,1/4,1/8)$	$16d(5/8,5/8,5/8)$
$M_x(\mu_B)$	0	0	0
$M_y(\mu_B)$	0.52(2)	0	0
$M_z(\mu_B)$	0.52(2)	0.59(5)	0
Moment(μ_B)	0.73(3)	0.59(5)	0
R_p(%)	5.46	6.97	7.19
R_{wp}(%)	7.31	9.02	9.25
χ^2	1.31	0.96	1.07

8, whereas the jump in the Co moment, if any, around 42 K is rather small, in agreement with the small volume change at the transition shown in Fig. 3, since the magnetovolume anomaly is directly proportional to the $M_{Co}{}^2$ in a first approximation for RCo_2 compounds.[7] The temperature dependence of the Nd moment is distinctly different from that reported in Ref. 11, in which the Nd moment varied smoothly and followed the Brillouin function for $J=9/2$. The present NPD work demonstrates that the magnetic and the structural transitions of $NdCo_2$ at 42 K involve changes not only in easy magnetization direction (EMD) but also in the magnitude of magnetization. It is also revealed that the magnetization jump of the bulk sample at 42 K is attributed essentially to the change of the EMD and that of the Nd moment.

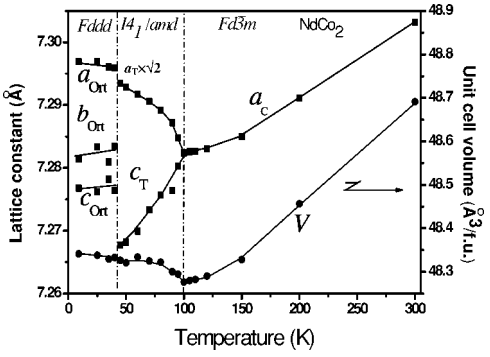

FIG. 3. Temperature dependence of the lattice constant and the unit cell volume of $NdCo_2$.

B. Magnetostriction

RCo_2 compounds exhibit a large anisotropic magnetostriction along the direction of magnetization, giving rise to large lattice distortions.[7] Within a first approximation the magnetostriction of a cubic crystal in any direction given by the direction cosines β_i can be expressed as

$$\lambda = (3/2)\lambda_{100}\left(\sum_i \alpha_i^2\beta_i^2 - 1/9\right) + 3\lambda_{111}\sum_{i<j}\alpha_i\alpha_j\beta_i\beta_j, \quad (1)$$

where the α_i's represent the direction cosines of the magnetization. The magnetostriction constants λ_{100} and λ_{111} are defined as the deformations along the [100] (i.e., [001] in the tetragonal structure) and [111] directions, respectively. From Eq. (1), one can obtain the following expression:

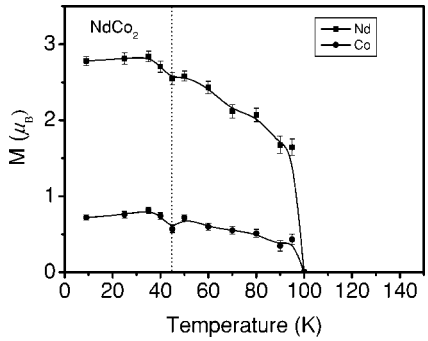

FIG. 4. Temperature dependence of magnetic moments of Nd and Co in $NdCo_2$. The errors bars are also shown. The solid lines are guides to the eye.

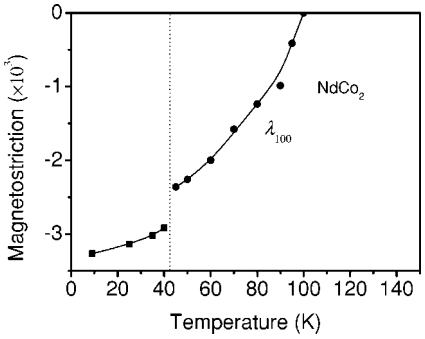

FIG. 5. Temperature dependence of the anisotropic magnetostriction constant λ_{100} of $NdCo_2$.

$$\lambda_{100} = \frac{2}{3}\Delta a/a, \tag{2}$$

where Δa is the difference between inequivalent edges of the distorted cube.[20] The obtained anisotropic magnetostriction λ_{100} at different temperature is shown in Fig. 5. The absolute value of λ_{100} decreases with temperature. An anomaly is revealed at about 42 K, where the first-order structural transition takes place. The obtained λ_{100} at 9 K is about -3.2×10^{-3}, which is a little smaller than the report of Gratz *et al.*[7]

The RCo_2 compounds show a large spontaneous volume magnetostriction due to the magnetic ordering of itinerant electron system. Thermal expansion measurements serve as a useful tool to study the *d*-electron magnetism in the RCo_2 compounds. The difference between the unit cell volume at a given temperature V_m and the "paramagnetic" unit cell volume V_p gives the spontaneous volume magnetostriction

$$\omega_s(T) = [V_m(T) - V_P(T)]/V_P(T), \tag{3}$$

where V_p is obtained by extrapolation from the paramagnetic temperature region. In a first approximation, Eq. (3) is related to the *d*-electron magnetic moment M_{Co} by $\omega_s = kCM_{\mathrm{Co}}^2$, where k is the isotropic compressibility and C is the volume magnetostriction coupling constant.[19] The obtained ω_s at 9 K is about 2.9×10^{-3}. From Fig. 4, M_{Co} is about $0.7\mu_B$. The value of kC is thus derived to be about $6.0\times10^{-3}\ \mu_B^{-2}$.

C. Field dependence of crystal structure

Figure 6 shows part of the NPD patterns recorded in zero field and in a field of 6.9 T. It is revealed that the cubic structure can be recovered by an applied magnetic field. The (800), (080), and (008) reflections for the orthorhombic structure at 10 K and the (440) and (008) reflections for the tetragonal structure at 50 K merge into a single (800) reflection for the cubic structure under the applied field of 6.9 T.

The splitting of the (620) reflection for the cubic structure is also salient as the lattice distortion occurs. The (620) reflection in the cubic structure splits into three reflections for the tetragonal structure, i.e., (420), (332), and (116), and into six reflections for the orthorhombic structure, i.e., (620), (602), (260), (062), (206), and (026). In the tetragonal structure the (420) and (332) reflections overlap severely, while in the orthorhombic structure the first four reflections, i.e., (620), (602), (260), and (062), also overlap severely (see the inset in Fig. 8). Figure 7 shows the field dependence of the relative intensity of $(116)_T$ reflection at 50 K, which indicates that at this temperature the tetragonal structure is transformed to the cubic structure at $H\sim0.26$ T. At 10 K, the total intensity I_S of the (206) and (026) reflections, with respect to the total intensity I_T of the six reflections, decreases rapidly for $H<0.6$ T as shown in Fig. 8. The profile evolution of the NPD patterns recorded at 10 K under the same experimental conditions except for the strength of the applied field is presented in the inset in Fig. 8. Figure 8 indicates that at 10 K a transition from the orthorhombic structure to the tetragonal structure occurs at $H\sim0.6$ T and a transition from the tetragonal structure to the cubic structure takes place at $H\sim2.9$ T. The profile evolution shown in the inset in Fig. 8 also ascertains the field-driven structural transitions. If the intensity decrease of the tetragonal $(116)_T$ peak or that of the orthorhombic (206) and (026) peaks were due to a field induced preferential orientation of the crystallites, the intensity of the peaks at lower angle should be increased accordingly.

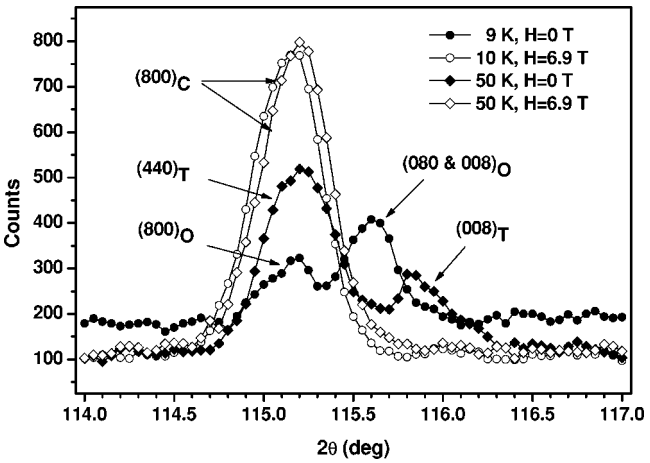

FIG. 6. NPD patterns at 10 and 50 K under zero field and 6.9 T.

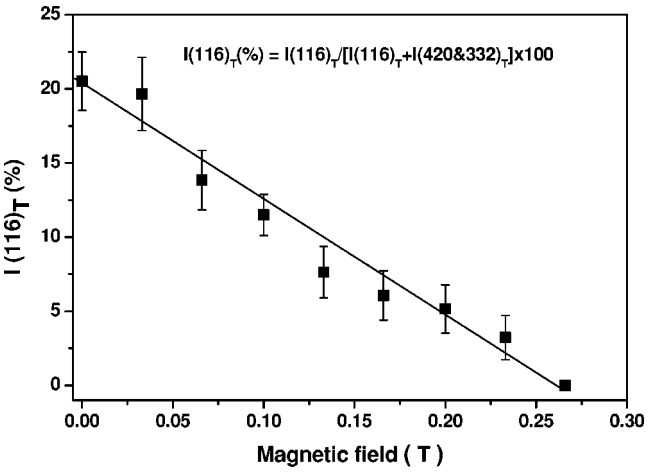

FIG. 7. Field dependence of the relative intensity of $(116)_T$ reflection of the tetragonal structure at 50 K.

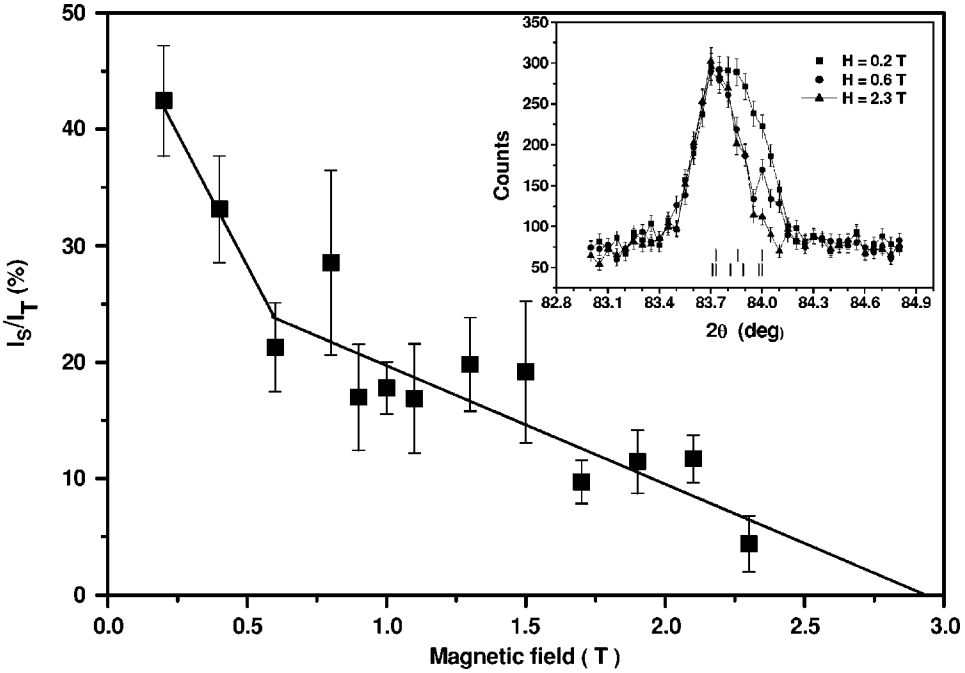

FIG. 8. Field dependence of the relative intensity of the (206) and (026) reflections for the orthorhombic structure at 10 K. I_S is the total intensity of the (206) and (026) reflections, I_T the total intensity of the (620), (602), (260), (062), (206), and (026) reflections. The inset shows the profiles of the NPD patterns at 10 K in magnetic fields of 0.2, 0.6, and 2.3 T. The vertical bars indicate the expected Bragg positions for tetragonal (420), (332), and (116) reflections (upper raw), and for (620), (602), (260), (062), (206), and (026) reflections, in sequence of increasing angle.

IV. DISCUSSION

The temperature dependence of lattice constants, anisotropic magnetostriction constant, and magnetic moments of $NdCo_2$ shown in Figs. 3–5 indicate that the magnetic and the structural transitions are second-order transitions in the vicinity of T_C and are first-order transitions around 42 K. Based on the data shown in Fig. 3, it is easy to derive the lengths of Nd-Nd, Nd-Co, and Co-Co bonds in the structure. Figure 9(a) illustrates the cubic Laves phase structure for $NdCo_2$ at room temperature and the coordination polyhedra of the Co atom and the Nd atom. Figure 9(b) presents the temperature dependence of the bondlengths of a Nd atom to its ligand atoms (4Nd+12Co) and of a Co atom to its ligand atoms (6Nd+6Co). In Fig. 9(b), d_{NdNd} is the length of the Nd-Nd bonds, $d_{\mathrm{NdCo}}(i)(i=a,b,c)$ the length of the Nd-Co bonds with the largest projection along the i direction and $d_{\mathrm{CoCo}}(ij)(i,j=a,b,c)$ the length of the Co-Co bonds along the $(i+j)$ or $(i-j)$ directions.

Figure 9(b) shows that d_{NdNd} varies smoothly as the temperature decreases, whereas $d_{\mathrm{NdCo}}(a)$ and $d_{\mathrm{NdCo}}(b)$ increase and $d_{\mathrm{NdCo}}(c)$ decreases obviously below T_C. At 42 K an abrupt decrease or increase occurs for $d_{\mathrm{NdCo}}(b)$ or $d_{\mathrm{NdCo}}(c)$. For d_{CoCo}, similar feature is observed, i.e., $d_{\mathrm{CoCo}}(ab)$ increases, $d_{\mathrm{CoCo}}(ac)$ and $d_{\mathrm{CoCo}}(bc)$ decrease below T_C, while an abrupt decrease or increase takes place for $d_{\mathrm{CoCo}}(ab)$ or $d_{\mathrm{CoCo}}(ac)$. Therefore, the coordination ployhedra of both the Nd and the Co atoms in the magnetic states are compressed in the easy magnetization direction for both the tetragonal and the orthorhombic structures.

Since d_{NdNd} does not exhibit any obvious jump at 42 K, the abrupt increase of Nd moment should be associated with the abrupt changes in length of the Nd-Co bonds. However, the average length d_{ave}(NdCo) of Nd-Co bonds is almost independent of temperature below T_C as indicated by the dashed line in Fig. 9(b). It implies that the abrupt increase of Nd moment is essentially due to the change in the chemical environment around Nd atoms. In the tetragonal structure a Nd atom involves in eight long and four short Nd-Co bonds to its ligand Co atoms, whereas in the orthorhombic structure it participates in four long and eight short Nd-Co bonds to its ligand Co atoms. Therefore, the spin reorientation due to the temperature dependence of the anisotropy energy results in the structural transition via strong magnetoelastic interaction, which in turn alters the crystal electric field (CEF) acting on Nd atoms and leads to the increase of the Nd moment. However, although the bondlengths of a Co atom to its ligand atoms (d_{NdCo} and d_{CoCo}) also change discontinuously at 42 K, the Co moment changes only slightly as shown in Fig. 4. This phenomenon is coincident with the metamagnetic character of the Co moment in RCo_2 compounds, which approaches to the saturated value of $0.8–1\mu_B$ rapidly once it is induced by the molecular-field or an external field.[1]

In the inset of Fig. 9(b) we show the temperature dependence of the strain on Nd-Co bonds measured by $\varepsilon = \langle (d_{\mathrm{NdCo}} - d_{\mathrm{ave}})^2 \rangle^{1/2} / d_{\mathrm{ave}}$. Below T_C, the strain increases pronouncedly as temperature decreases and as the long-range magnetic ordering develops, indicative of a strong magnetic exchange striction. A magnetic exchange striction results from a geometrical degree of freedom which allows the two coupled ions to accommodate their distance in order to gain magnetic exchange energy at the expense of elastic energy.[21,22] The strain is partially released by the structural transition and almost independent of the temperature below 42 K. It implies the exchange energy gain by the striction is negligible in the orthorhombic structure and the magnetocrystalline anisotropy dominates the stable magnetic structure. For the tetragonal $NdCo_2$, in which the exchange striction is strong, an applied field can release the lattice strain by gaining Zeeman energy to recover the cubic symmetry. For the orthorhombic $NdCo_2$, however, an applied field first

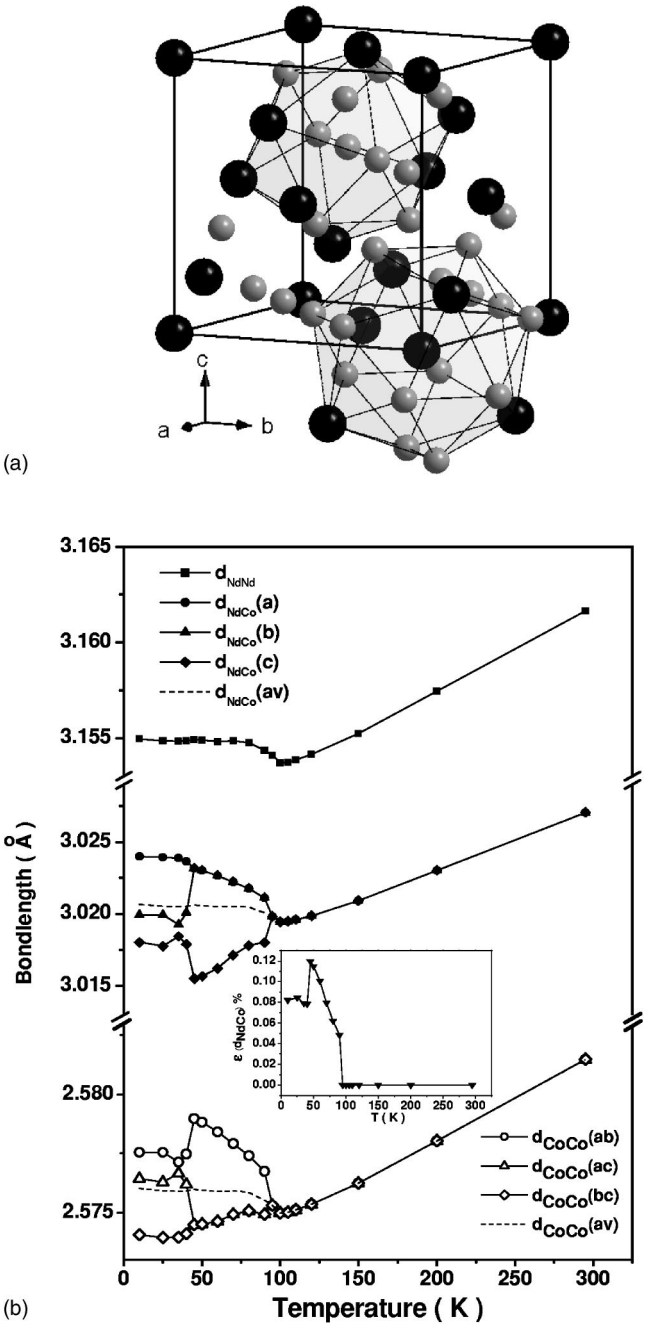

FIG. 9. (a) Crystal structure of the cubic Laves phase for $NdCo_2$ at room temperature. The coordination polyhedra of the Nd and the Co atoms are depicted. (b) Temperature dependence of the lengths of Nd-Nd, Nd-Co, and Co-Co bonds between the centered and the ligand atoms in the coordination polyhedra of the Nd and the Co atoms. The dashed lines represent the averaged lengths of the bonds. The inset in (b) shows the relative strain on the Nd-Co bonds.

drove the system to a less distorted tetragonal symmetry at relatively low field and then recovered the cubic symmetry at a much higher field than that required for the tetragonal phase, since the exchange striction is week below 42 K.

Recalling that a much higher field, ~6.5 T, than that for recovering the cubic structure, ~2.9 T at 10 K, was required to smear out the magnetization jump at 42 K,[12] it is anticipated that the easy magnetic magnetization direction does not alter although the cubic structure is recovered. It implies that the simultaneous magnetic and structural transitions observed at zero field can be decoupled by a relatively modest applied field. Similar phenomenon was also reported in monoclinic $Tb_5Si_2Ge_2$,[15] in which a field-induced paramagnetic to ferromagnetic transition could occur without the structural transition that usually accompanies the magnetic transition in other $R_5(Si,Ge)_4$ systems.[13,14] However, because of the cubic symmetry and the influence of the applied magnetic field, it is not possible to determine the accurate magnetic structure by powder-neutron diffraction, and similar field-dependent neutron diffraction works on single crystals are desired. Unfortunately, we have not got high-quality single crystals for the NPD experiments under our experimental conditions.

V. CONCLUSIONS

The crystal structure, magnetic structure, and anisotropic magnetostriction of $NdCo_2$ have been investigated by means of temperature- and field-dependent high-resolution neutron-powder diffraction. $NdCo_2$ has the cubic Laves-phase $C15$ structure above Curie temperature T_C(~100 K). With decreasing temperature, $NdCo_2$ undergoes a second-order transition from the cubic to a tetragonal structure (space group $I4_1/ama$) at T_C and a first-order transition from the tetragonal to an orthorhombic structure (space group $Fddd$) at $T \approx 42$ K. The temperature dependence of the magnetic moment and the anisotropic magnetostriction constant is determined by neutron powder diffraction. The Nd moment and the magnetostriction exhibit abrupt changes at 42 K, indicative of a strong coupling between magnetism and crystal structure. Analysis of bondlength reveals a strong magnetic exchange striction in the tetragonal structure and a dominating contribution of magnetocrystalline anisotropy in the orthorhombic structure. The structural transition at T_C is attributed to the strong magnetoelastic interaction, whereas the structural transition at 42 K is caused via the magnetoelastic interaction by the spin reorientation due to the temperature dependence of the anisotropy energy. The structural transition at 42 K alters the crystal electric field acting on the Nd atoms, leading to the increase of the Nd moment. The cubic symmetry of the structure can be recovered below T_C by an application of relatively modest magnetic fields, indicating a decoupling of the magnetic and crystal structural transitions under the applied magnetic fields.

ACKNOWLEDGEMENTS

This work was supported by the National Natural Science Foundation of China, the State Key Project of Fundamental Research, the National "863" project, and the exchange program between NIST and Chinese Academy of Sciences.

*E-mail address: ghrao@aphy.iphy.ac.cn

[1] N. H. Duc and P. E. Brommer, in *Handbook of Magnetic Materials*, edited by K. H. J. Buschow (North-Holland, Amsterdam, 1999), Vol. 12, p. 259.
[2] M. I. Batashevich, H. A. Katori, T. Goto, H. Wada, T. Maeda, T. Mori, and M. Shiga, Physica B **229**, 315 (1997).
[3] T. Goto, H. A. Katori, T. Sakakibara, H. Mitamura, K. Fukamichi, and K. Murata, J. Appl. Phys. **76**, 6682 (1994).
[4] T. Goto, K. Fukamichi, and H. Yamada, Physica B **300**, 167 (2001).
[5] S. Khmelevskyi and P. Mohn, J. Phys.: Condens. Matter **12**, 9453 (2000).
[6] E. Gratz and A. S. Markosyan, J. Phys.: Condens. Matter **13**, R385 (2001).
[7] E. Gratz, A. Lindbaum, A. S. Markosyan, H. Mueller, and A. Y. Sokolou, J. Phys.: Condens. Matter **6**, 6699 (1994).
[8] E. Gratz, Solid State Commun. **48**, 825 (1983).
[9] U. Atzmony, M. P. Dariel, and G. Dublon, Phys. Rev. B **14**, 3713 (1976).
[10] R. M. Moon and W. C. Koehler, J. Appl. Phys. **36**, 978 (1965).
[11] P. Hendy and E. W. Lee, Phys. Status Solidi A **50**, 101 (1978).
[12] N. Baranov, E. Gratz, H. Nowotny, and W. Steiner, J. Magn. Magn. Mater. **37**, 206 (1983).
[13] V. K. Pecharsky and K. A. Gschneidner, Jr., Phys. Rev. Lett. **78**, 4494 (1997).
[14] V. K. Pecharsky and K. A. Gschneidner, Jr., Adv. Mater. (Weinheim, Ger.) **13**, 683 (2001).
[15] L. Morellon, C. Ritter, C. Magen, P. A. Algarabel, and M. R. Ibarra, Phys. Rev. B **68**, 024417 (2003).
[16] H. M. Rietveld, Acta Crystallogr. **229**, 151 (1967).
[17] J. L. Rodríguez-Carvajal, Physica B **192**, 55 (1993).
[18] Z. W. Ouyang, G. H. Rao, H. F. Yang, W. F. Liu, and J. K. Liang, Appl. Phys. Lett. **81**, 97 (2002).
[19] K. H. J. Buschow, in *Ferromagnetic Materials*, edited by E. P. Wohlfarth (North-Holland, Amsterdam, 1980), Vol. 7, p 297.
[20] R. Z. Levitin and A. S. Markosyan, J. Magn. Magn. Mater. **84**, 247 (1990).
[21] C. Kittel, Phys. Rev. **120**, 335 (1960).
[22] Th. Strässle, F. Juranyi, M. Schneider, S. Janssen, A. Furrer, K. W. Krämer, and H. U. Güdel, Phys. Rev. Lett. **92**, 257202 (2004).